Density-fluctuation spectra of dilute mixtures of ^{3}He in superfluid ^{4}He

M. Lücke
Institut für Festkörperforschung der Kernforschungsanlage Jülich, Postfach 1913, D-5170 Jülich, West Germany

A. Szprynger
Institute of Low Temperature and Structure Research, Polish Academy of Sciences, 50-950 Wroclaw, P.O.B. 937, Poland

(Received 25 June 1981; revised manuscript received 2 April 1982)

The density-fluctuation spectra $S_{ij}(k,\omega)$ $(i,j=3,4)$ are evaluated with a matrix dispersion-relation representation in terms of characteristic frequencies and complex self-energies by the incorporation of damping via decay into ^{3}He quasiparticle-quasihole excitations and by the use of renormalized fluctuation frequencies. The hybridization of ^{4}He rotons with ^{3}He quasiparticle excitations is too small to induce a peak splitting in $S_{44}(k,\omega)$ at the level crossing while the effective phonon-roton exchange potential between ^{3}He quasiparticles splits the spectrum $S_{33}(k,\omega)$ into two peaks. The energy shift of the main neutron scattering intensity with respect to pure ^{4}He agrees semiquantitatively with experiments. It is caused by partly competing effects listed in the order of their importance: frequency changes induced by the altered structure of ^{4}He in the mixture, coupling between ^{4}He and ^{3}He restoring forces, hybridization with ^{3}He quasiparticle-quasihole excitations, and the contribution of $S_{34}(k,\omega)$. Decay into two-mode density excitations is investigated within a mode-coupling approximation.

I. INTRODUCTION

The density excitation spectrum[1] of a dilute mixture of ^{3}He in superfluid ^{4}He is an interesting experimental problem and a challenge for many-body theories of strongly interacting fermions and bosons. Research activities have been directed mostly towards determining the dispersion $\epsilon_3^0(k)$ of a single ^{3}He atom in He II.[2–10] The resulting picture is that, due to the strong ^{3}He-^{4}He bare interaction, the ^{3}He atom "polarizes" the ^{4}He bath, and, surrounding itself by a "cloud" of density excitations, becomes a quasiparticle. The effective mass increases weakly with wave numbers[8–10] in such a way that $\epsilon_3^0(k)$ slightly bends over near the roton minimum of the ^{4}He single-mode dispersion[11] $\epsilon_4^0(k)$ without forming a minimum.[4] The ^{3}He quasiparticle excitation is undamped[9,10] since ^{4}He is superfluid: The gap $\epsilon_4^0(k)$ in the bath's excitation spectrum kinematically prevents the quasiparticle from dissipating energy.[9,12] As $\epsilon_3^0(k)$ approaches the energy threshold[5,9,10,12] for roton emission, an undamped ^{3}He quasiparticle excitation is no longer possible, spectral weight is transferred to a continuum of damped excitations[9] at larger frequencies, and the dispersion $\epsilon_3^0(k)$ terminates at the threshold.[9,12] That is well understood in terms of the decay of a ^{3}He excitation into a ^{4}He roton and a ^{3}He quasiparticle.

The picture for the density-fluctuation spectra of a mixture of, say, 6% ^{3}He concentration is less clear. Of course, the intensity under the formerly sharp peak of the ^{3}He quasiparticle excitation is spread over a "band" (at least its lower edge is presumably well defined) of quasiparticle-quasihole excitations. And, more importantly, the ^{4}He density-fluctuation spectrum is changed by the presence of macroscopically many ^{3}He atoms. Earlier conclusions[13] about large roton energy shifts inferred from indirect measurements were disproven by scattering experiments.[14–16]

Nonetheless, the density-fluctuation spectra, in particular near the crossing of the ^{3}He quasiparticle-quasihole excitation band with the ^{4}He single-mode dispersion, are still a challenge. The few theoretical attempts made in this direction were focused on evaluating roton line broadening and roton energy shifts produced by decay into and hybridization with ^{3}He quasiparticle-quasihole excitations within various theoretical frameworks.[7,17]

Common to them is that the shift of the ^{4}He single-mode excitation energy is due to the repulsion of ^{4}He and ^{3}He levels; i.e., it is upwards to the left of the crossing where $\epsilon_4 > \epsilon_3$ and downwards to the right where $\epsilon_4 < \epsilon_3$. This disagrees, at least partly, with neutron scattering data[15,16] since the more important effect of the changed ^{4}He structure in the mixture on the restoring force against a ^{4}He density fluctuation has been neglected. The structurally induced frequency shifts turn out to have the opposite sign of the level repulsion and furthermore, are mostly larger than the level repulsion.

The purpose of this work is to evaluate these and other features of the density-fluctuation spectra $S_{ij}(k,\omega)$ $(i,j=3,4)$. To accomplish this, we use a dispersion-relation representation of the 2×2 matrix of density response functions $\chi_{ij}(k,z)$ (Sec. II) in terms of a characteristic frequency matrix of static restoring forces and a complex k- and z-dependent self-energy matrix. A generalized Feynman model (Sec. III) shows already the importance of structurally induced frequency shifts and of the restoring force coupling via off-diagonal elements of the characteristic frequency matrix. This wave-number–dependent coupling strength is expressed (Appendix A) in terms of structure functions, which are input in our theory. In Sec. IV we introduce renormalized fluctuation frequencies and incorporate damping by decay into ^{3}He quasiparticle-quasihole excitations. We elucidate in quantitative detail hybridizations, peak splitting, energy shifts, and linewidths, and we compare the above-mentioned static effects upon the fluctation spectra with the dynamical effect due to hybridization of excitations. We determine the size of various effects causing the main peak of the total neutron scattering intensity of the mixture to be shifted with respect to pure ^{4}He and compare our results with experiments. In Appendix C we investigate decay into two-mode density fluctuations and its influence on the spectra. The last section gives a discussion of our results that are obtained without any adjustable parameters.

All numerical calculations refer to number density fluctuations in a 6% mixture at zero temperature. Thus we ignore the incoherent contribution from spin density fluctuations to the total neutron scattering intensity, which is proportional to

$$S_{\rm tot}(k,\omega)=(1-x)S_{44}(k,\omega)+2\left[x(1-x)\frac{\sigma_3}{\sigma_4}\right]^{1/2}S_{34}(k,\omega)+x\frac{\sigma_3}{\sigma_4}S_{33}(k,\omega)+x\frac{\sigma_3^{\rm inc}}{\sigma_4}S_{33}^{\rm inc}(k,\omega) \tag{1.1}$$

for a mixture of concentration $x=N_3/(N_3+N_4)$. The ratio of coherent cross sections $\sigma_3/\sigma_4=4.34$ is about 4 times larger than $\sigma_3^{\rm inc}/\sigma_4=1.06$ (Ref. 18), and the size of $S_{33}^{\rm inc}(k,\omega)$ in a dilute mixture is presumably at most comparable with $S_{33}(k,\omega)$ (in an ideal Fermi gas they are the same). Thus it seems reasonable to neglect the fourth term of (1.1) in comparison with the third, which itself is less important than the first two.

II. DENSITY RESPONSE OF ^{3}He-^{4}He MIXTURES

The fluctuation dynamics of the two particle number densities

$$\rho_j(\vec{k},t)=\frac{1}{\sqrt{N_j}}\sum_{n_j=1}^{N_j}e^{-i\vec{k}\cdot\vec{r}_{n_j}(t)},\quad j=3,4 \tag{2.1}$$

are conveniently described in terms of the symmetric 2×2 matrix of complex density response functions, reading in standard notation[19,20]

$$\chi_{ij}(k,z)=\pm i\int_{-\infty}^{\infty}dt\,\Theta(\pm t)e^{izt}\langle[\rho_i(-\vec{k},t),\rho_j(\vec{k})]\rangle \quad \text{for Im } z\gtrless 0 \tag{2.2a}$$

$$=\int_{-\infty}^{\infty}\frac{d\omega}{\pi}\frac{\chi_{ij}''(k,\omega)}{\omega-z}\,. \tag{2.2b}$$

The spectral functions $\chi_{ij}''(k,\omega)$ are the imaginary parts of (2.2) along the real frequency axis,

$$\chi(k,\omega\pm i0)=\chi'(k,\omega)\pm i\chi''(k,\omega)\,, \tag{2.3}$$

and $\chi_{ij}'(k,\omega)$ are the corresponding real parts. The matrix $\chi_{ij}''(k,\omega)$ is positive semidefinite for $\omega\geq 0$, and all

its elements are odd in frequency. They are related via the fluctuation-dissipation theorem to the dynamic structure factors $S_{ij}(k,\omega)$ determining the neutron scattering intensity. In the zero-temperature limit one has

$$S_{ij}(k,\omega)=2\Theta(\omega)\chi''_{ij}(k,\omega)\ . \tag{2.4}$$

As in other many-body problems it is advantageous to use a dispersion-relation representation for the matrix of response functions

$$\chi(k,z)=-[z^2-\Omega^2(k)+z\Sigma(k,z)]^{-1}k^2m^{-1} \tag{2.5}$$

in terms of complex self-energies $\Sigma_{ij}(k,z)$ and a characteristic frequency matrix of restoring forces

$$\Omega^2(k)=k^2m^{-1}\chi^{-1}(k)=\frac{1}{1-W^2(k)}\begin{pmatrix}\omega_3^2(k) & -(\frac{4}{3})^{1/2}W(k)\omega_3(k)\omega_4(k)\\ -(\frac{3}{4})^{1/2}W(k)\omega_3(k)\omega_4(k) & \omega_4^2(k)\end{pmatrix}. \tag{2.6}$$

Here m denotes the diagonal matrix of bare masses m_3,m_4. For convenience we have expressed $\Omega^2(k)$ in terms of squared frequencies,

$$\omega_i^2(k)=\frac{k^2}{m_i\chi_{ii}(k)}\ , \tag{2.7}$$

which measure the $z=0$ restoring forces of ^{3}He and ^{4}He density fluctuations via static susceptibilities

$$\chi_{ij}(k)=\chi_{ij}(k,z=0)=\int_{-\infty}^{\infty}\frac{d\omega}{\pi}\frac{\chi''_{ij}(k,\omega)}{\omega}\ . \tag{2.8}$$

The restoring forces $\omega_i(k)$ are coupled with a wave-number–dependent strength

$$W(k)=\chi_{34}(k)/\sqrt{\chi_{33}(k)\chi_{44}(k)}\ , \tag{2.9}$$

which is proportional to the square root of the mean densities $\sqrt{n_3n_4}$. The coupling also enhances the restoring forces to $\omega_i(k)/[1-W^2(k)]^{1/2}$. Note that $\chi_{ij}^2\le\chi_{ii}\chi_{jj}$.

In order to give an idea of the size of the characteristic frequencies (2.7) to those readers unfamiliar with them, we mention that in the ideal Fermi gas, $\omega_{\rm FG}(k)$ lies for wave numbers $k\gg 2k_F$ in the center of the particle-hole excitation band. For smaller k it approaches a linear dispersion $\omega_{\rm FG}(k<k_F)\sim kv_F/\sqrt{3}$, which is within the band. To obtain a first estimate of

$$\omega_4^2(k)=\omega_4^{02}(k)\chi^0_{44}(k)/\chi_{44}(k)\ , \tag{2.10}$$

one might ignore the quotient of static ^{4}He susceptibilities in pure ^{4}He and in the mixture and observe that the characteristic frequency[21] $\omega_4^0(k)$ of pure ^{4}He lies for all wave numbers closer[12] to the single-mode dispersion[21] $\epsilon_4^0(k)$ than the Feynman frequency:

$$\epsilon_4^0(k)\le\omega_4^0(k)\le k^2/2m_4S^0_{44}(k)\ .$$

In particular, $\omega_4^0(k\to 0)=c_4^0k$ yields[22] the correct sound velocity.

The positive-semidefinite matrix $\Sigma''_{ij}(k,\omega)$ of imaginary parts of

$$\Sigma(k,\omega+i0)=\Sigma'(k,\omega)+i\Sigma''(k,\omega) \tag{2.11}$$

reflects all dissipative mechanisms by which density fluctuations of frequency ω and wave number k decay, while the real parts $\Sigma'_{ij}(k,\omega)$ lead to renormalization of fluctuation frequencies. The imaginary parts are even in ω, whereas the real parts are odd. Economical and powerful approximations reflecting the two-component nature of the mixture are best made within the 2×2 matrix formalism for $\Sigma_{ij}(k,z)$ rather than for the self-energies $\sigma_{33}(k,z),\sigma_{44}(k,z)$, which appear in the single-component representation of

$$\chi_{44}(k,z)=\frac{-k^2/m_4}{z^2-\omega_4^2(k)+z\sigma_{44}(k,z)}\ , \tag{2.12}$$

or similarly of $\chi_{33}(k,z)$. Section III (Apendix B) demonstrates how elaborate $\sigma_{33}(k,z)$ must be to ensure properties obtained within the 2×2 matrix framework from a (nearly) trivial approximation to $\Sigma_{ij}(k,z)$. For future reference we mention that the self-energies can formally be expressed[20,23] as resolvent matrix elements

$$\Sigma_{ij}(k,z)=\left\langle\rho_i(\vec{k})\left|\mathscr{L}^2Q\frac{1}{Q\mathscr{L}Q-z}Q\mathscr{L}^2\right|\rho_j(\vec{k})\right\rangle\frac{m_j}{k^2} \tag{2.13}$$

with a scalar product between operators A,B defined by their static susceptibility

$$(A\mid B)=\chi_{AB}(z=0)=i\int_0^\infty dt\,\langle[A^\dagger(t),B]\rangle\ . \tag{2.14}$$

The time evolution $A(t)=e^{i\mathcal{L}t}A$ is determined by the Liouville operator $\mathcal{L}A(t)=[H,A(t)]$. The projector Q projects orthogonally to densities $\rho_i(\vec{k})$ and currents $\mathcal{L}\rho_i(\vec{k})$ of ^{3}He and ^{4}He.

The statistical dynamics of ^{4}He density fluctuations in mixtures are modified according to (2.5) by three effects: (1) The static restoring force $\omega_4(k)$ differs from that of pure ^{4}He by the quotient $[\chi^0_{44}(k)/\chi_{44}(k)]^{1/2}$, reflecting mostly the structural change of ^{4}He in the mixture. This is the main cause[24] for the (small) roton energy shift in dilute mixtures at low temperatures.[16] (2) There is a second characteristic frequency $\omega_3(k)$ to which $\omega_4(k)$ is coupled via $W(k)$. This induces resonance shifts in the density-fluctuation spectra via the off-diagonal as well as via the diagonal elements of the static restoring force matrix Ω^2. (3) In the mixture there are additional dissipative mechanisms to which density fluctuations couple at least in a restricted range of wave numbers and frequencies. That implies enhanced decay rates described by the imaginary parts $\Sigma''_{ij}(k,\omega)$ and modified frequency renormalization via the real parts $\Sigma'_{ij}(k,\omega)$.

Although the effects are not independent—restoring forces, decay rates Σ'' and real parts Σ' determine the fluctuation spectra $\chi''_{ij}(k,\omega)$, which in turn self-consistently determine static susceptibilities and the coupling to dissipative mechanisms—it is instructive to investigate them separately. The generalized Feynman model, e.g., eliminates effect (3) by taking $\Sigma=0$.

III. GENERALIZED FEYNMAN MODEL—UNDAMPED DENSITY FLUCTUATIONS

The density response

$$\chi(k,z)=-[z^2-\Omega^2(k)]^{-1}k^2m^{-1} \tag{3.1}$$

obtained from the simplest approximation, $\Sigma_{ij}(k,z)=0$, displays already a large amount of the characteristic features of the mixture. First of all, there are two frequencies characterizing the system. The spectra ($\omega\geq 0$)

$$\chi''_{ij}(k,\omega)/\pi=Z^+_{ij}(k)\delta(\omega-\epsilon_+(k))+Z^-_{ij}(k)\delta(\omega-\epsilon_-(k)) \tag{3.2}$$

consist of two δ functions of strength

$$Z^{\pm}(k)=\frac{\pm k^2/2}{\epsilon_+(k)-\epsilon_-(k)}\times[1-\epsilon_{\mp}(k)\Omega^{-1}(k)]m^{-1}, \tag{3.3}$$

where $\epsilon^2_{\pm}(k)$ are the eigenvalues of the positive-semidefinite matrix $\Omega^2(k)=\Omega(k)\cdot\Omega(k)$.

The form of Eqs. (3.1)–(3.3) yields the correct f sum rule of the spectra

$$\int_0^\infty \frac{d\omega}{\pi}\chi''(k,\omega)=\tfrac{1}{2}k^2m^{-1}, \tag{3.4}$$

and in addition, the choice

$$\Omega(k)=\tfrac{1}{2}k^2m^{-1}S^{-1}(k) \tag{3.5}$$

enforces the density response's having the correct total spectral weight

$$S_{ij}(k)=\int_0^\infty \frac{d\omega}{\pi}\chi''_{ij}(k,\omega). \tag{3.6}$$

As in pure ^{4}He, one can also expect here the choice $\Omega^2(k)=k^2m^{-1}\chi^{-1}(k)$ enforcing the correct static susceptibilities to be superior[12] to the conventional Feynman-type approximation (3.5). Unfortunately, the static susceptibilities $\chi_{ij}(k)$ of the mixture are not known.

The two excitation levels $\omega_{F4}=k^2/2m_4S_{44}(k)$ and $\omega_{F3}=k^2/2m_3S_{33}(k)$ cross (cf. Fig. 1) at wave number $k_c=1.64$ Å^{-1} and energy 21.8 K, if the structure functions as given in Appendix A are used. Owing to the coupling described by the off-diagonal elements of Ω there is a level splitting $\epsilon_+(k_c)-\epsilon_-(k_c)=0.4$ K. The upper (lower) level ϵ_+ (ϵ_-) represents density fluctuations of ^{4}He (^{3}He) for wave numbers $k<k_c$, while for $k>k_c$ the converse is true: The spectral weights Z_{44} and

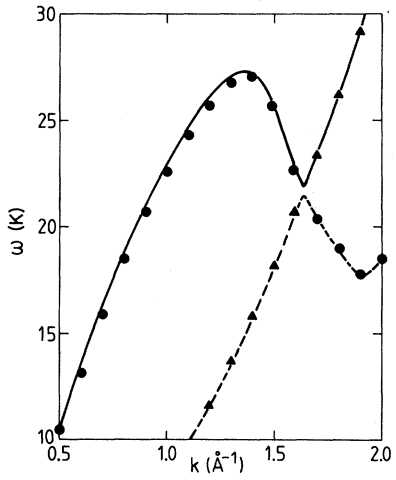

FIG. 1. Excitation energies $\epsilon_+(k)$ (full curve) and $\epsilon_-(k)$ (dashed curve) of undamped density fluctuations in the mixture obtained from the generalized Feynman model. Closed circles denote $k^2/2m_4S_{44}(k)$ and triangles $k^2/2m_3S_{33}(k)$.

Z_{33}^{+} (Z_{44}^{+} and Z_{33}^{-}) are vanishingly small below (above) k_c. The level repulsion induced by the coupling pushes, for wave numbers $k < k_c$, the ^{4}He (^{3}He) excitation energy ϵ_+ (ϵ_-) to higher (lower) values than ω_{F4} (ω_{F3}). For $k > k_c$, on the other hand, the ^{4}He (^{3}He) excitation levels ϵ_- (ϵ_+) are shifted downwards (upwards). The upward resonance shifts are mostly of the order of 0.3 K while the downward shifts, being less than about 0.1 K, cannot be seen in Fig. 1

However, the net shift of ^{4}He excitation energies in the mixture with respect to those in pure ^{4}He, ω_{F4}^0, does not follow this simple level-repulsion scheme. For some wave numbers the different structure of ^{4}He in the mixture having the opposite effect on the characteristic ^{4}He frequency overcompensates the level repulsion. At $k=2$ Å^{-1}, for example, $\omega_{F4}-\omega_{F4}^0 \simeq 0.3$ K, so that the net shift $\epsilon_- - \omega_{F4}^0 \simeq 0.2$ K is upwards, whereas with repulsion alone it would be downwards, $\simeq -0.1$ K.

Thus the generalized Feynman model shows the importance of the changed ^{4}He structure. It also yields an estimate of the absolute size of the net shift of ^{4}He fluctuation energies in the mixture. Its main drawback is the incorrect wave number and frequency scale: ^{3}He and ^{4}He levels do not cross around the roton but rather at too small a wave number, $k_c = 1.64$ Å^{-1}, and too high an energy. Thus the repulsive shift, already changing sign at k_c, has a wrong wave-number dependence compared to the structurally induced frequency shift. In summary, the foremost deficiency is the absence of the proper renormalization of excitation frequencies ($\Sigma' = 0$) rather than the absence of damping ($\Sigma'' = 0$).

IV. ^{4}He SINGLE-MODE EXCITATIONS AND ^{3}He QUASIPARTICLE-QUASIHOLE EXCITATIONS

In this section we (i) appropriately renormalize the fluctuation frequencies and (ii) include decay of density fluctuations into ^{3}He quasiparticle-quasihole excitations by choosing $\Sigma_{33}''(k,\omega)$ correspondingly. We neglect the off-diagonal elements of the self-energy matrix as well as $\Sigma_{44}''(k,\omega)$ in view of the small roton decay rate of 0.06 K measured[25] for a 6% mixture at $T=0.25$ K. The real part $\Sigma_{44}'(k,\omega)$ is approximately taken care of by replacing the "bare" restoring force $\omega_4(k)$ by a renormalized frequency $\epsilon_4(k)$ obtained as follows.

A. The renormalized frequency $\epsilon_4(k)$

In pure ^{4}He the bare restoring force $\omega_4^0(k)$ is renormalized by the real part of the self-energy according to the relation[12,26]

$$\epsilon_4^{0\,2}(k) = \omega_4^{0\,2}(k) - \epsilon_4^0(k)\Sigma_{44}^{0\prime}(k,\epsilon_4^0(k)) , \tag{4.1}$$

which determines the energy $\epsilon_4^0(k)$ of the undamped single-mode excitation. In the mixture, however, we must replace ω_4 by the frequency $\epsilon_4 = \epsilon_4^0 + d\epsilon_4$, which is shifted in comparison with ϵ_4^0 already as a result of the difference $d\omega_4 = \omega_4 - \omega_4^0$ in the bare restoring forces even if one ignores for the sake of simplicity that the real part of the self-energy will be different as well. Doing just that,

$$d\epsilon_4(k) \simeq \frac{\partial \epsilon_4^0(k)}{\partial \omega_4^0(k)} d\omega_4(k) \tag{4.2}$$

is determined by $d\omega_4(k)$ and by the partial derivative

$$\frac{\partial \epsilon_4^0(k)}{\partial \epsilon_4^0(k)} = 2\omega_4^0(k)\left[\omega + \frac{[\omega_4^0(k)]^2}{\omega} + \omega\frac{\partial \Sigma_{44}^{0\prime}(k,\omega)}{\partial \omega}\right]^{-1}_{\omega=\epsilon_4^0(k)} = 2\omega_4^0(k)\frac{Z_4^0(k)}{k^2/m_4} , \tag{4.3}$$

which is obtained from (4.1) in terms of the single-mode excitation strength[21,22] $Z_4^0(k)$ or pure ^{4}He. As a side remark we mention that relations (4.3) are exact.[12,26]

Thus we replace the bare restoring force $\omega_4(k)$ of ^{4}He density fluctuations by the renormalized $\epsilon_4(k)$,

$$\omega_4(k) \to \epsilon_4(k) = \epsilon_4^0(k) + 2\frac{Z_4^0(k)}{k^2/m_4}[\omega_4^0(k)]^2\left[\frac{\omega_4(k)}{\omega_4^0(k)} - 1\right] , \tag{4.4}$$

and evaluate the quotient

$$\omega_4(k)/\omega_4^0(k) \simeq S_{44}^0(k)/S_{44}(k) \tag{4.5}$$

within a Feynman approximation which faithfully reflects the structural effects that are mainly responsible for the change of the restoring forces.

B. ^{3}He quasiparticle excitations

The remaining approximations for $\omega_3(k)$ and $\Sigma_{33}(k,z)$ are motivated as follows. A single ^{3}He atom moves almost without friction,[27] as in a mechanical vacuum, in the superfluid bath but with a dispersion $\epsilon_3^0(k) = k^2/2m_3^*(k)$ determined by

a slightly wave-number–dependent effective mass.[8–10] Thus, in view of the dilution, we describe the ^{3}He subsystem as an ideal Fermi gas of quasiparticles with a mean effective mass $\bar{m}_3^* \simeq 2.65 m_3$, averaged for our purposes over the wave number range up to roton momenta, and replace $\omega_3(k)$ and $\Sigma_{33}(k,z)$ by the corresponding quantities of an ideal Fermi gas of mass $\bar{m}_3^*$:

$$\omega_3^2(k) \to \omega_{\rm FG}^2(k) = \frac{k^2}{\bar{m}_3^* \chi_{\rm FG}(k)} , \tag{4.6}$$

$$z^2 + z\Sigma_{33}(k,z) \to z^2 + z\Sigma_{\rm FG}(k,z) = \omega_{\rm FG}^2(k)[1 + \pi_{\rm FG}^{-1}(k,z)] . \tag{4.7}$$

The self-energy is given in terms of the reduced polarization operator

$$\pi_{\rm FG}(k,z) = -\chi_{\rm FG}(k,z)/\chi_{\rm FG}(k) , \tag{4.8}$$

which describes particle-hole excitations. Inserting all this into the matrix formula (2.5) one finds that the ^{3}He density response is of a random-phase approximation (RPA) type:

$$\chi_{33}(k,z) = \frac{\bar{m}_3^*}{m_3} \frac{\chi_{\rm FG}(k,z)}{1 - V_{\rm eff}(k,z)\pi_{\rm FG}(k,z)} . \tag{4.9a}$$

The coupling $W(k)$ between the restoring forces against density fluctuations causes a k,z dependent effective potential between ^{3}He quasiparticles

$$V_{\rm eff}(k,z) = \gamma^2(k) \frac{z^2}{z^2 - \tilde{\epsilon}_4^2(k)} ,$$

$$\gamma^2(k) = \frac{W^2(k)}{1 - W^2(k)} \tag{4.9b}$$

which is induced and mediated by the exchange of undamped phonon-roton excitations of the ^{4}He bath with energy

$$\tilde{\epsilon}_4(k) = \epsilon_4(k)/[1 - W^2(k)]^{1/2} . \tag{4.10}$$

The potential $V_{\rm eff}(k,z)$, which is analogous and similar to the Fröhlich phonon-exchange potential between electrons,[28,29] is proportional to the mean number densities $n_3 n_4$ via $W^2(k)$ [see Eq. (A2)].

C. ^{4}He density fluctuations

The coupling $W(k)$ also leads to a polarization potential for ^{4}He density fluctuations, reflecting the fact that they can decay into (interacting) ^{3}He quasiparticle-quasihole excitations:

$$\chi_{44}(k,z) = \frac{-k^2/m_4}{z^2 - \tilde{\epsilon}_4^2(k)[1 + \gamma^2(k)\pi(k,z)]} . \tag{4.11}$$

The vertex is proportional to $\gamma(k)$ and thus to $\sqrt{n_3 n_4}$. The decay is kinematically possible within the band

$$\frac{k^2}{2\bar{m}_3^*} - kv_F \le \omega \le \frac{k^2}{2\bar{m}_3^*} + kv_F , \tag{4.12}$$

where the imaginary part of the polarization operator

$$\pi(k,z) = \pi_{\rm FG}(k,z)[1 - \gamma^2(k)\pi_{\rm FG}(k,z)]^{-1} , \tag{4.13}$$

determined by the particle-hole "bubble" $\pi_{\rm FG}(k,z)$, is nonzero. The cross susceptibilities

$$\chi_{34}(k,z) = -(\tfrac{3}{4})^{1/2}\gamma(k)\chi_{33}(k,z) \times \frac{\omega_{\rm FG}(k)\tilde{\epsilon}_4(k)}{z^2 - \tilde{\epsilon}_4^2(k)} \tag{4.14}$$

are "almost" products of $\chi_{33}(k,z)$ and $\chi_{44}(k,z)$ in this model.

That the above approximations properly reflect the decay of a ^{4}He single-mode excitation into ^{3}He excitations can be inferred from a comparison with the ^{4}He density response in the single-component representation (2.12). A standard mode-coupling approximation (Appendix B) for its self-energy $\sigma_{44}(k,z)$ by which ^{4}He density modes and ^{3}He quasiparticles are explicitly coupled leads to the expression (4.11). Similarly, one recovers (Appendix B) Eqs. (4.9) for the ^{3}He density response.

D. Density-fluctuation spectra

To evaluate the spectra of Eqs. (4.9)–(4.14) we need the ideal Fermi-gas functions for a particle mass $\bar{m}_3^* = 2.65 m_3$, the coupling function $W(k)$ [Eq. (A2)], and to determine $\epsilon_4(k)$ also $S_{44}^0(k)/S_{44}(k)$ [Eqs. (A4)], $Z_4^0(k)$, $\omega_4^0(k)$, and $\epsilon_4^0(k)$. The last three quantities were not taken from experiments but rather from a previous theory.[26] Its single-mode dispersion $\epsilon_4^0(k)$ overestimates the roton energy by about 2.3 K. We found that to be irrelevant for the ^{4}He energy shifts in the mixture, whether they are induced structurally or dynamically by decay into quasiparticle-quasihole excitations. We used the results[26] (i) to be consistent with the ^{3}He quasiparticle excitation energy $\epsilon_3^0(k)$ obtained[9] with the ^{4}He response spectrum of Ref. 26, and (ii) to compare with the mode-coupling theory of Appendix C in which the self-energies are evaluated with the spectra $\chi_{44}^{0\prime\prime}(k,\omega)$ (Ref. 26) and $\chi_{33}^{0\prime\prime}(k,\omega)$ (Ref. 9).

In our model, all density fluctuations are damped only within the quasiparticle-quasihole excitation band [Eq. (4.12); thin lines in Fig. 2]. The frequency $\omega_{FG}(k)$ [Eq. (4.6); dashed line in Fig. 2] is practically in the center of the band. Outside the band all response spectra $\chi''_{ij}(k,\omega)$ display a δ-function spike at the frequency (dots outside the band) where the determinant of the inverse susceptibility matrix (2.5) vanishes. While the δ function carries practically the total spectral weight of $\chi''_{44}(k,\omega)$, the weight of $\chi''_{33}(k,\omega)$ is negligible outside the band, so we drew open triangles denoting the upper peak positions of $\chi''_{33}(k,\omega)$ only within the band. The lower peak (▲) of $\chi''_{33}(k,\omega)$ carries for small k almost the total spectral weight of ^{3}He density fluctuations. Approaching the roton position in ωk plane from below its dispersion (▲) bends over (without forming a minimum), and more and more weight is transferred to the upper peak (△). The lower (upper) peak remains always below (above) the energy $\tilde{\epsilon}_4(k)$ where $\chi''_{33}(k,\omega)$ has a zero because of the diverging phonon-roton exchange potential (4.9b). This peak splitting in the spectrum $\chi''_{33}(k,\omega)$,[24] which is about 1.2 K around roton momenta, is due to the hybridization of a ^{3}He quasiparticle-quasihole excitation with a ^{4}He single-mode excitation. The latter is virtually emitted and reabsorbed by the former, thus giving rise to the exchange potential. The spectrum $\chi''_{34}(k,\omega)$ changes sign at $\omega=\tilde{\epsilon}_4(k)$ but otherwise resembles[24] $\chi''_{33}(k,\omega)$, which is obvious from Eq. (4.14).

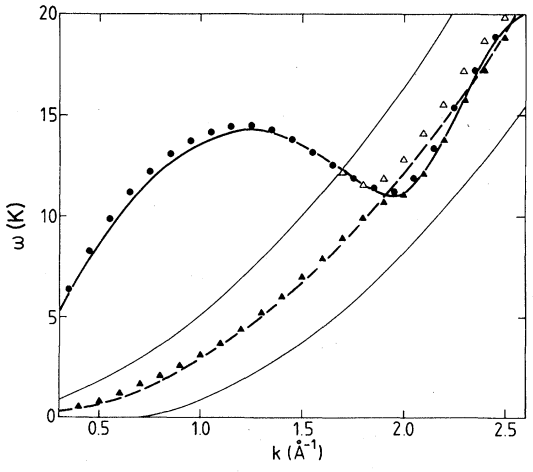

FIG. 2. Peak position (closed circles) of the total neutron scattering intensity $S_{tot}(k,\omega)$ (1.1) compared with the single-mode excitation energy $\epsilon^0_4(k)$ (Ref. 26) of pure ^{4}He (full thick curve). Triangles denote peak positions of $\chi''_{33}(k,\omega)$ and the dashed line, $\omega_{FG}(k)$ [Eq. (4.6)]. The thin lines are the boundaries (4.12) of the ^{3}He quasiparticle-quasihole excitation band.

The spectrum $\chi''_{44}(k,\omega)$ has practically only one peak, indicated (approximately) by solid circles in Fig. 2. For all wave numbers shown there, the vertex $\gamma(k)$ for decay of ^{4}He density fluctuations into ^{3}He quasiparticle-quasihole excitations is too small to induce an additional zero of the denominator in (4.11) at a real frequency other than that at $\omega\simeq\tilde{\epsilon}_4(k)$ and marked (approximately) by solid circles. Only for smaller k, where that zero is outside the band, does $\chi''_{44}(k,\omega)$ have a small side maximum in the band somewhat above its center. However, as soon as the former [closed circle at $\omega\simeq\tilde{\epsilon}_4(k)$] enters the band around $k=1.7$ Å^{-1} the side maximum disappears by merging into the low-frequency wing of the main peak at $\omega\simeq\tilde{\epsilon}_4(k)$. Thus, in particular around roton wave numbers, $\chi''_{44}(k,\omega)$ displays only one peak[24]: The polarization potential $\gamma^2(k)\pi'(k,\omega)$ due to virtual quasiparticle-quasihole excitations is too small to cause a detectable hybridization of a roton with the latter.

E. Energy shifts

The position (closed circles in Fig. 2) of the main peak in the total neutron scattering law $S_{tot}(k,\omega)$ differs very little from the single-mode dispersion $\epsilon^0_4(k)$ (solid curve) in pure ^{4}He. The enlarged frequency scale of Fig. 3 reveals an oscillatory behavior of the energy shift caused by various, partly competing effects (1)–(4) listed below in the order of their importance. The first two are of static origin and the remaining of dynamic origin.

(1) The first effect due to the different structure of ^{4}He in the mixture dominates the other three. The structural difference enters via the difference $d\epsilon_4(k)$ (dash-dot line in Fig. 3) of the ^{4}He fluctuation frequencies which in turn is dominated by the difference $d\omega_4(k)$ of the "bare" restoring forces. The partial derivative $\partial\epsilon^0_4(k)/\partial\omega^0_4(k)$ entering $d\epsilon_4(k)$ as well is almost wave-number independent, about 0.6 in the range 1–2.2 Å^{-1}, and then it drops rapidly to zero because $Z^0_4(k>2.2\ \text{Å}^{-1})\to 0$.[21,26] Thus the wave-number dependence of $d\epsilon_4(k)$ [Eq. (4.4)] is dictated by the relative difference $S^0_{44}(k)/S_{44}(k)-1$ of the structure factors which changes sign around $k\simeq 1.9$ Å^{-1}. The altered structure of ^{4}He in the mixture has been invoked earlier[16] to explain ^{4}He energy differences by

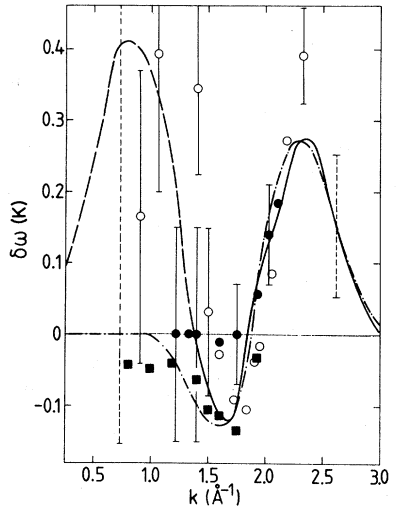

FIG. 3. Shift of the peak position of $S_{tot}(k,\omega)$ (1.1) with respect to the single-mode excitation energy of pure ^{4}He (full curve and dashed curve) compared with neutron scattering results of Hilton *et al.* (Ref. 16) obtained for a 6% mixture at $T=0.75$ K (closed circles), $T=0.6$ K (squares), and of Rowe *et al.* (Ref. 15) (open circles) obtained for $x=5\%$ at $T=1.6$ K. Error bars of the experiments (solid vertical lines) and from uncertainties of input data entering theory (dashed vertical lines) are shown as well. The dash-dot curve denotes the shift $d\epsilon_4(k)$ (4.4). See text for further information.

shifting the roton dispersion curve towards a smaller wave number, thereby accounting for the increased ^{4}He interatomic distance in the mixture. In view of the above discussion it is not surprising that this rather crude procedure captures the essence of the structurally induced energy shifts in the immediate roton surrounding. Figure 3 shows that $d\epsilon_4(k)$ (dash-dot line) is almost identical to the peak shift (solid line) of $S_{tot}(k,\omega)$ above $k\simeq 1.5$ Å^{-1}. The differences are due to effects (2)–(4).

(2) The coupling $W(k)$ to the ^{3}He restoring force enhances the fluctuation frequency $\epsilon_4(k)$ towards $\tilde{\epsilon}_4(k)$ [Eq. (4.10)] thus inducing upwards energy shifts which are typically less than 0.05 K. However, below $k\simeq 1.25$ Å^{-1}, where $W^2(k)$ as well as $\epsilon_4(k)$ is relatively large, this enhancement is large enough to dominate the other effects and cause the large upward shift of the dashed part of the curve in Fig. 3, which will be discussed later on.

(3) The frequency $\tilde{\epsilon}_4(k)$ is further renormalized by the polarization potential $\gamma^2(k)\pi(k,z)$, which is produced by and reflects the decay into ^{3}He quasiparticle-quasihole excitations. The real part of the potential causes a level repulsion between $\tilde{\epsilon}_4(k)$ and the center frequency $k^2/2\bar{m}_3^*$ of the quasiparticle excitation band: For k smaller (larger) than about 1.9 Å^{-1}, where both levels cross, $\tilde{\epsilon}_4(k)$ is larger (smaller) than $k^2/2\bar{m}_3^*$ and consequently the position of the main peak of $\chi''_{44}(k,\omega)$ is pushed towards a larger (smaller) frequency than $\tilde{\epsilon}_4(k)$. Thus the energy shift induced by the repulsion between ^{4}He fluctuation energies, and ^{3}He quasiparticle excitation levels is opposite to the structurally induced shift $d\epsilon_4(k)$ (dash-dot line in Fig. 3) which is negative (positive) for wave numbers smaller (larger) than $k\simeq 1.9$ Å^{-1}. However, the repulsion effect is small—at most 0.06 K—compared to the structural effect (1).

(4) The last effect is due to the cross spectrum $\chi''_{34}(k,\omega)$ [Eq. (4.14)] being positive below the frequency $\tilde{\epsilon}_4(k)$, in the immediate vicinity of which $\chi''_{44}(k,\omega)$ has its main peak, and negative above. That causes the total neutron scattering intensity $S_{tot}(k,\omega)$ [Eq. (1.1)] to be slightly asymmetric[24] and also to have a peak at a lower frequency than the peak position of $\chi''_{44}(k,\omega)$. The downward shift is quite small, mostly about 0.01 K with a maximum of 0.03 K at $k=2.2$ Å^{-1}.

The difference of the peak position of $S_{tot}(k,\omega)$ with respect to $\epsilon_4^0(k)$ resulting from the combination of the above four effects is shown in Fig. 3 by the solid (and dashed) line. It agrees semiquantitatively with neutron scattering results (closed circles, squares, and open circles). The latter also reflect thermal effects which are absent in our calculation. The uncertainties of our input parameters—experimental errors of $S_{44}(k)$ and an assumed uncertainty of $S_{34}(k)$ of about 50% (cf. Appendix A)—cause uncertainties (dashed vertical lines in Fig. 3) of our theoretical results exceeding 100% for smaller wave numbers. In that case our theoretical energy shifts are less reliable, which is indicated by the dashed part of the energy shift curve in Fig. 3.

Since the peak widths of $S_{tot}(k,\omega)$ are uncertain by more than 100% we did not show them here. Nevertheless we would like to mention that they compare semiquantitatively with experiments: The half-width at half maximum of the roton peak in the total neutron scattering intensity from a 6% mixture was reported to be broadened with respect to pure ^{4}He by $\delta\Gamma=0.15$ K at $T=0.6$ K (Ref. 30) and by $\delta\Gamma=0.06$ K at $T=0.25$ K (Ref. 25) while our result is $\delta\Gamma=0.1$ K.

V. DISCUSSION

Our investigation of number density fluctuations in a dilute ^{3}He-He II mixture with a dispersion-

relation representation of the 2×2 matrix of density-response functions $\chi_{ij}(k,z)$ in terms of a characteristic frequency matrix of static restoring forces and a complex k,z dependent self-energy matrix $\Sigma_{ij}(k,z)$ gave the following results.

The ^{4}He density fluctuations in the mixture differ from those in pure ^{4}He because of three effects: (1) The bare restoring force $\omega_4(k)$ given by the susceptibility against static ^{4}He density perturbations is altered by the different structure of ^{4}He in the mixture. (2) The static coupling via the off-diagonal elements of the characteristic frequency matrix causes a repulsion of ^{3}He and ^{4}He excitation levels. The coupling strength $W(k)$ expressed by equal-time structure functions is rather small, $-0.25\lesssim W(k)\lesssim 0.1$. (3) Density fluctuations of the mixture couple to additional damping mechanisms, causing enhanced decay rates and additional frequency renormalization via hybridization with the decay states.

A generalized Feymman model ($\Sigma=0$) gives first estimates of the relative importance of effects (1) and (2). However, the wave number and frequency scale of its unrenormalized fluctuation frequencies, in particular the position of the ^{3}He-^{4}He level crossing, is wrong. Introducing properly renormalized energies and incorporating damping by decay into ^{3}He quasiparticle-quasihole excitations via $\Sigma_{33}(k,z)$ we obtained a theory which, without adjustable parameter, gives (i) a transparent explanation of the fluctuation spectra of the mixture and (ii) semiquantitative agreement with neutron scattering experiments.

The resulting ^{3}He density response is of RPA type: Between the ^{3}He quasiparticles acts a k- and z-dependent effective potential, which is generated by exchange of (undamped) ^{4}He single-mode excitations similar to the Fröhlich phonon-exchange potential of electrons in metals. The strength, determined by $W(k)$, is not a fit parameter. This hybridization of ^{3}He quasiparticles with ^{4}He single modes causes the density-fluctuation spectrum $S_{33}(k,\omega)$ to have two peaks. One is for all wave numbers above, the other one below the ^{4}He single-mode dispersion. Approaching the latter's roton mininum, the lower peak's dispersion bends over and follows it without forming a minimum or a flat plateau. Simultaneously, more and more spectral weight is transferred to the upper peak. The peak splitting of $S_{33}(k,\omega)$ around roton momenta is $\simeq$1.2 K.

^{4}He density fluctuations feel a polarization potential produced by decay into ^{3}He quasiparticle-quasihole excitations. However, their hybridization with a ^{4}He single mode is too weak to induce a peak splitting in the spectrum $S_{44}(k,\omega)$ since the decay vertex determined by $W(k)$ is too small. Our roton linewidth due only to decay into quasiparticle-quasihole excitations agrees surprisingly well with the experimental low-temperature roton line broadening in the mixture. (However, the reliability of our width is obliterated by input uncertainties of the structure functions entailing, via the vertex, considerable uncertainty in the decay rate.) Decay into two-mode density fluctuations described by (a restricted class of) mode-coupling diagrams in leading order of the concentration changes the spectra only in minor details except near the crossing of ^{4}He and ^{3}He excitation levels. There two-mode decay causes complex, partly competing dynamical couplings and hybridizations via the various self-energies which to describe properly requires a more complete and self-consistent treatment.

The peak position of the total neutron scattering intensity is shifted in comparison to that of pure ^{4}He by two static and two dynamic effects. The largest is due to the structurally induced frequency shift of the restoring force against ^{4}He density fluctuations. The repulsion of ^{4}He fluctuation energies and ^{3}He quasiparticle-quasihole excitation levels is opposite to and smaller than the structurally induced shifts. The static coupling of ^{4}He and ^{3}He restoring forces enhances the fluctuation frequencies thus inducing shifts that are small around roton momenta but become larger for wave numbers around the maximum of the ^{4}He dispersion. Finally, the contribution of the cross spectrum to the total scattering intensity induces additional shifts since $\chi''_{34}(k,\omega)$ changes sign at the ^{4}He single-mode excitation energy.

All effects combined yield rather small shifts of the dominant peak in the total neutron scattering intensity which agree semiquantitatively with the experimental results obtained at the lowest temperatures. In particular the upward energy shift for wave numbers larger than the roton momentum is a result of the altered ^{4}He structure in the mixture, whereas level repulsion alone yields a small downward shift.

ACKNOWLEDGMENT

One of us (A.S.) gratefully acknowledges the hospitality of the Institut für Festkörperforschung der Kernforschungsanlage Jülich.

APPENDIX A: COUPLING STRENGTH $W(k)$, STRUCTURE FUNCTIONS $S_{ij}(k)$

Here we evaluate the coupling strength $W(k)$ (2.9) between static restoring forces for density fluctuations within the generalized Feynman model.

Although that is a crude approximation to the spectra, the frequency integrals $\chi_{ij}(k)$ (2.8) entering $W(k)$ are somewhat insensitive to details of the spectral distribution. This is supported by two such different systems as an ideal Fermi gas and pure ^{4}He. The standard Feynman approximation for the latter yields a static susceptibility $4m_4[S^0_{44}(k)/k]^2$ with the exact long-wavelength behavior $(m_4c_4^{02})^{-1}$. Its largest deviation (about 40%) from the experimental susceptibility[21] $\chi^0_{44}(k)$ occurs at $k=2$ Å^{-1}. However, the overall shape agrees very well with $\chi^0_{44}(k)$. The same kind of approximation for the ideal Fermi gas yields a static susceptibility $4m[S_{\rm FG}(k)/k]^2$ which is almost identical with $\chi_{\rm FG}(k)$ above $2k_F$ while its largest deviation (25%) occurs at $k=0$. Again the shape of the two curves is almost identical.

We thus conclude that the approximation [(3.1) and (3.5)]

$$\chi_{ij}(k)=k^2[\Omega^{-2}(k)m^{-1}]_{ij} =\frac{4}{k^2}[S(k)mS(k)]_{ij} \tag{A1}$$

of the susceptibilities ensures a realistic estimate of the coupling function

$$W(k)=\frac{\chi_{34}(k)}{\sqrt{\chi_{33}(k)\chi_{44}(k)}} \simeq\frac{S_{34}(m_3S_{33}+m_4S_{44})}{\sqrt{(m_3S_{33}^2+m_4S_{34}^2)(m_3S_{34}^2+m_4S_{44}^2)}}, \tag{A2}$$

even more so since $W(k)$ is determined by a quotient of susceptibilities. Note that the coupling is proportional to the square root of the mean number densities $\sqrt{n_3n_4}$ via $S_{34}(k)$.

The structure functions $S_{ij}(k)$ are needed as input. For $S_{33}(k)$ we use the structure function

$$S_{\rm FG}(k)=\begin{cases}\frac{3}{4}\frac{k}{k_F}\left[1-\frac{1}{12}\left[\frac{k}{k_F}\right]^2\right] & \text{for } k\le 2k_F\\ 1 \quad \text{otherwise}\end{cases} \tag{A3}$$

of an ideal Fermi gas of density n_3 occurring in the 6% mixture for which $2k_F=0.67$ Å^{-1}. The cross-correlation function $S_{34}(k)$ is taken from the work of Massey *et al.*[31] which "yields reliable estimates of $S_{34}(k)$ for the binary boson solution in the region of intermediate and high k."[32] For smaller k we modified $S_{34}(k)$ of Massey *et al.* as shown in Fig. 4 to obtain physical meaningful eigenvalues $\epsilon_\pm(k)$ of $\Omega(k)=\frac{1}{2}k^2m^{-1}S^{-1}(k)$ (cf. Sec. III) which are consistent with the results in the region of intermediate and large wave numbers. Since $S_{34}(k)$ enters directly into the coupling function $W(k)$ (A2) and determines its size and shape (cf. Fig. 4), it is highly desirable to have more reliable information on $S_{34}(k)$.

$S_{44}(k)$ can, in principle, be extracted from the experimentally determined[33] total x-ray scattering intensity $S(k)$ of a mixture if the contributions $xS_{33}(k)$ and $2\sqrt{x(1-x)}S_{34}(k)$ were reliably known. Since that is far from being true we ignored them within a small-concentration approximation altogether in

$$\frac{S_{44}(k)}{S^0_{44}(k)}=\frac{S(k)}{S^0_{44}(k)}\left[1-2\left[\frac{x}{1-x}\right]^{1/2}\frac{S_{34}(k)}{S(k)} +\frac{x}{1-x}\left[1-\frac{S_{33}(k)}{S(k)}\right]\right], \tag{A4}$$

and thus used the experimental $S(k)/S^0_{44}(k)$ (closed circles in Fig. 4) as input for $S_{44}(k)/S^0_{44}(k)$ (solid curve in Fig. 4). The structure function $S^0_{44}(k)$ of pure ^{4}He was taken from the works of Achter and Meyer[34] and Hallock.[35]

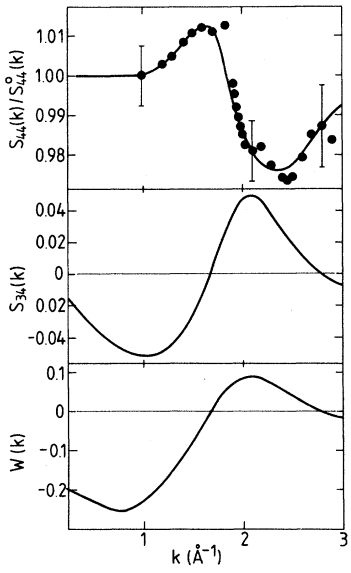

FIG. 4. Input functions (full curves) used in this work. See text for further information.

APPENDIX B: MODE COUPLING APPROXIMATION TO SELF-ENERGIES IN SINGLE-COMPONENT REPRESENTATION

Instead of using the 2×2 matrix formulation we derive here the approximations (4.9) and (4.11) within the single-component representation (2.12) of the density response functions $\chi_{ii}(k,z)$ and then make a mode-coupling approximation for the self-energies,

$$\sigma_{ii}(k,z)=\left[\rho_i(\vec{k})\left|\mathscr{L}^2Q_i\frac{1}{Q_i\mathscr{L}Q_i-z}Q_i\mathscr{L}^2\right|\rho_i(\vec{k})\right]\frac{m_i}{k^2}\ . \tag{B1}$$

The above projectors differ from the one in (2.13) since Q_4 projects out only ρ_4 and $\mathscr{L}\rho_4$ but *not* ρ_3, and vice versa for Q_3. Furthermore, ρ_3 (ρ_4) is a slow mode of the mixture, its fluctuation frequency is comparable to that of ^{4}He (^{3}He) density fluctuations, and both are coupled, e.g., via $\mathscr{L}^2\rho_i$. Thus the dissipation spectrum $\sigma''_{44}(k,\omega)$ [$\sigma''_{33}(k,\omega)$] contains a damping mechanism whereby ^{4}He (^{3}He) density-fluctuation energy is transferred directly to ρ_3 (ρ_4) excitations. Only this decay channel of ^{4}He fluctuations is considered here. Following the standard procedure of mode-coupling theory[12,26,36,37] we project in (B1) on the slow mode ρ_3

$$\sigma_{44}(k,z)\simeq\frac{(\rho_4\,|\,\mathscr{L}^2Q_4\,|\,\rho_3)}{(\rho_3\,|\,\rho_3)}\left[\rho_3\left|\frac{1}{\mathscr{L}-z}\right|\rho_3\right]\frac{(\rho_3\,|\,Q_4\mathscr{L}^2\,|\,\rho_4)}{(\rho_3\,|\,\rho_3)}\frac{m_4}{k^2} \tag{B2}$$

to obtain

$$z\sigma_{44}(k,z)\simeq\omega_2^2(k)W^2(k)\times[\chi_{33}(k,z)/\chi_{33}(k)-1]\ . \tag{B3}$$

The second term in (B3) reflects a restoring force enhancement caused by the coupling between the modes. In addition to the analogous mode-coupling contribution to $\sigma_{33}(k,z)$, reflecting decay of ^{3}He excitations into a ^{4}He density mode, we allow the former also to decay into ^{3}He particle-hole excitations by adding the free gas self-energy (4.7),

$$z\sigma_{33}(k,z)\simeq\omega_3^2(k)W^2(k)\times[\chi_{44}(k,z)/\chi_{44}(k)-1]+z\Sigma_{\rm FG}(k,z)\ . \tag{B4}$$

In the resolvent of (B2) we have ignored the projector Q_4 which suppresses the excitation of a ρ_4 mode by the Liouville operator in $(Q_4\mathscr{L}Q_4-z)^{-1}\rho_3(\vec{k})$. We approximately account for this restriction of the resolvent by replacing the susceptibility quotients of (B3) and (B4),

$$\chi_{44}(k,z)/\chi_{44}(k)\to-\omega_4^2(k)/[z^2-\omega_4^2(k)]\ ,\qquad \chi_{33}(k,z)/\chi_{33}(k)\to\chi_{\rm FG}(k,z)/\chi_{\rm FG}(k)\ , \tag{B5}$$

by the expressions obtained in the limit $W\to0$ in which the modes ρ_3 and ρ_4 are decoupled. As in Sec. IV we replace the bare restoring force $\omega_4(k)$ by the renormalized one $\epsilon_4(k)$,$\omega_3(k)$ by the ideal Fermi-gas frequency $\omega_{\rm FG}(k)$, and we evaluate the Fermi-gas functions for a particle mass $\bar{m}_3^*$. Then the resulting response functions $\chi_{ii}(k,z)$ coincide with (4.9) and (4.11) if $W^2(k)$ is small. That is the case for all wave numbers since $W^2(k)\leq0.06$ (Appendix A). Hence this mode-decay approximation which couples ρ_3 and ρ_4 modes via self-energies $\sigma_{ii}(k,z)$ yields the same response $\chi_{ii}(k,z)$ as the 2×2 matrix formalism wherein the fluctuation are coupled via off-diagonal elements of the restoring force matrix.

APPENDIX C: DECAY INTO TWO-MODE EXCITATIONS

Here we investigate decay into two-mode excitations as described by the product

$$B_{\vec{p}}(\vec{k};lm)=\tfrac{1}{2}[\delta\rho_l(\vec{p})\delta\rho_m(\vec{k}-\vec{p})+\delta\rho_m(\vec{p})\delta\rho_l(\vec{k}-\vec{p})] \tag{C1}$$

of two number density fluctuation operators with $l,m=3,4$. Within a mode-coupling approximation[9,12,26] we determine the two-mode contributions

$$\Sigma''_{ij}(k,\omega)\,|_{\text{2-mode}}\simeq\frac{m_j}{k^2}\sum_{\vec{p},\vec{p}'}\sum_{\substack{l,m\\l',m'}}V_{\vec{p}}(\vec{k};i\Longleftrightarrow lm)\psi''_{\vec{p}\,\vec{p}'}(\vec{k},\omega;lm,l'm')V_{\vec{p}'}(\vec{k};j\Longleftrightarrow l'm') \tag{C2}$$

to the damping rate $\Sigma''_{ij}(k,\omega)$ (2.13) by projecting onto the product "states" (C1). Thereby one obtains the

vertices

$$V_{\vec{p}}(\vec{k};i \Longleftrightarrow lm)=\sum_{\vec{p}'}(\rho_i(\vec{k}) \mid \mathscr{L}^2 Q \mid B_{\vec{p}'}(\vec{k};lm))[(B \mid B)^{-1}]_{\vec{p}',\vec{p}} . \tag{C3}$$

The spectrum of the two-mode propagator

$$\psi_{\vec{p}\,\vec{p}'}(\vec{k},z;lm,l'm')\simeq\left(\rho_l(\vec{p})\rho_m(\vec{k}-\vec{p})\left|\frac{1}{\mathscr{L}-z}\right|\rho_{l'}(\vec{p}\,')\rho_{m'}(\vec{k}-\vec{p}\,')\right) \tag{C4}$$

is evaluated by factorizing

$$\psi''(\vec{k},\omega)=\frac{1}{2\omega}\int_{-\infty}^{\infty}dt\, e^{i\omega t}\langle[\delta\rho_m^*(\vec{k}-\vec{p},t)\delta\rho_l^*(\vec{p},t),\delta\rho_{l'}(\vec{p}\,')\delta\rho_{m'}(\vec{k}-\vec{p}\,')]\rangle . \tag{C5}$$

That yields

$$\psi''_{\vec{p}\,\vec{p}'}(\vec{k},\omega;lm,l'm')\simeq\frac{1}{2\omega}\int_{-\infty}^{\infty}\frac{d\epsilon}{\pi}[\mathrm{sgn}(\epsilon)+\mathrm{sgn}(\omega-\epsilon)][\chi''_{ll'}(p,\epsilon)\chi''_{mm'}(\mid\vec{k}-\vec{p}\mid,\omega-\epsilon)\delta_{\vec{p}\,\vec{p}'}$$
$$+\chi''_{lm'}(p,\epsilon)\chi''_{ml'}(\mid\vec{k}-\vec{p}\mid,\omega-\epsilon)\delta_{\vec{p},\vec{k}-\vec{p}'}] \tag{C6}$$

upon use of the fluctuation dissipation theorem. In this work we neglect the decay corresponding to the vertices $V(3\Longleftrightarrow 44),V(4\Longleftrightarrow 33),V(3\Longleftrightarrow 33)$. The first two are small since $\mathscr{L}^2\rho_3$ (ρ_4) has no overlap with the two-mode operator $B(44)$ [$B(33)$]—$(\rho_3\mid\mathscr{L}^2\mid B(44))=0=(\rho_4\mid\mathscr{L}^2\mid B(33))$—and the last two vertices are small because of the small ^{3}He concentration. The remaining two-mode contributions (C6) to $\Sigma''_{ij}(k,\omega)$ (C2) are shown in Fig. 5 where a "bubble" diagram represents a particular convolution of response spectra multiplied by vertices. Here we will also neglect convolutions with a cross spectrum $\chi''_{34}(k,\omega)$ which is indefinite for positive frequencies. Thus we are left with the four digrams (a)—(d) in Fig. 5.

Since a ^{4}He density fluctuation can emit a ^{3}He density fluctuation only in the presence of a macroscopic amount of ^{3}He, the contributions of (c) and (d) vanish for small concentration x; the vertex $V(4\Longleftrightarrow 34)$ is proportional to $\sqrt{x}$. On the other hand, a ^{4}He density fluctuation can be generated by a single ^{3}He atom; the vertex $V(3\Longleftrightarrow 34)$ is finite for $x\to 0$. The concentration dependence of the vertices is easily seen by observing first that

$$(\rho_3(\vec{k})\mid\mathscr{L}^2\mid B_{\vec{p}}(\vec{k};34))=\frac{1}{\sqrt{V}}\frac{1}{2m_3}\vec{k}\cdot\frac{\vec{p}S_{34}(\mid\vec{k}-\vec{p}\mid)+(\vec{k}-\vec{p})S_{34}(p)}{\sqrt{n_3}} \tag{C7}$$

is finite for $N_3\to 1$ since

$$S_{ij}(k)=\langle\delta\rho_i^*(\vec{k})\delta\rho_j(\vec{k})\rangle=\delta_{ij}+\sqrt{n_i n_j}\int d\vec{r}\,e^{-i\vec{k}\cdot\vec{r}}[g_{ij}(r)-1] . \tag{C8}$$

[Equation (C7) does not pose a problem[38] in the thermodynamic limit $N_4\to\infty, V\to\infty$, $N_4/V\to n_4$; the factor $1/V$ from the square of the vertices is compensated by the density of states $V/(2\pi)^3$ in the wave-vector integration.] On the other hand,

$$\frac{(\rho_4(\vec{k})\mid\mathscr{L}^2\mid B_{\vec{p}}(\vec{k};34))}{(\rho_3(\vec{k})\mid\mathscr{L}^2\mid B_{\vec{p}}(\vec{k};34))}=\frac{m_3}{m_4}\left[\frac{N_3}{N_4}\right]^{1/2} \tag{C9}$$

vanishes in the thermodynamic limit for a finite number of ^{3}He atoms. Since, furthermore, the projector Q in (C3) does not modify the concentration dependence (C9), we approximate the vertex $V(4\Longleftrightarrow 34)$ by

$$V_{\vec{p}}(\vec{k};4\Longleftrightarrow 34)\simeq\frac{3}{4}\left[\frac{x}{1-x}\right]^{1/2}V_{\vec{p}}(\vec{k};3\Longleftrightarrow 34) . \tag{C10}$$

Then the diagrams (c) and (d) in Fig. 5 are given by diagram (b) multiplied by the appropriate concentra-

tion-dependent factor stemming from (C10). Thus we have to evaluate only diagrams (a) and (b).

To that end we used the response spectra $\chi''^{0}_{44}(k,\omega)$, $\chi''^{0}_{33}(k,\omega)$ of pure[26] ^{4}He and of a single ^{3}He atom in ^{4}He,[9] respectively, instead of determining χ''_{ij} in the self-energies self-consistently. Also the vertices $V(4 \Longleftrightarrow 44)$ (Ref. 26) and $V(3 \Longleftrightarrow 34)$ (Ref. 9) were evaluated in the limit of vanishing ^{3}He concentration. Then the self-energy matrix reads

$$\Sigma_{ij}(k,z) \simeq \begin{bmatrix} \Sigma_{\mathrm{FG}}(k,z)+\Sigma^0_{33}(k,z) & 0 \\ 0 & \Sigma^0_{44}(k,z) \end{bmatrix} + \Sigma^0_{33}(k,z) \begin{bmatrix} 0 & \left[\frac{x}{1-x}\right]^{1/2} \\ \frac{3}{4}\left[\frac{x}{1-x}\right]^{1/2} & \frac{3}{4}\left[\frac{x}{1-x}\right] \end{bmatrix}, \tag{C11}$$

where $\Sigma^0_{33}(k,z)$ is the self-energy[9] for a single ^{3}He atom in ^{4}He and $\Sigma^0_{44}(k,z)$ that of pure ^{4}He.[26] Decay into quasiparticle-quasihole excitations is also approximately described here by the self-energy (4.7) of an ideal Fermi gas of mass $\bar{m}^*_3$.

For the restoring force $\omega_3(k)$ we used $\omega^0_3(k)$ as obtained in Ref. 9, and $\omega_4(k)$ was approximated by $\omega^0_4(k)S^0_{44}(k)/S_{44}(k)$ (4.5) with $\omega^0_4(k)$ taken from Ref. 26. In contrast to Sec. IV we use here bare restoring forces $\omega_i(k)$ since the frequency renormalization has to come from $\Sigma'(k,\omega)$. We verified that neglecting diagrams (c) and (d) of Fig. 5, i.e., the second terms in (C11), yields practically the same peak positions of χ''_{33} and χ''_{44} as obtained in Sec. IV. This justifies the introduction of the renormalized frequencies in Sec. IV to account for the real parts associated with the diagrams of Figs. 5(a) and 5(b).

Including all labeled diagrams of Fig. 5 one finds that the spectra $\chi''_{ij}(k,\omega)$ resulting from (C11)

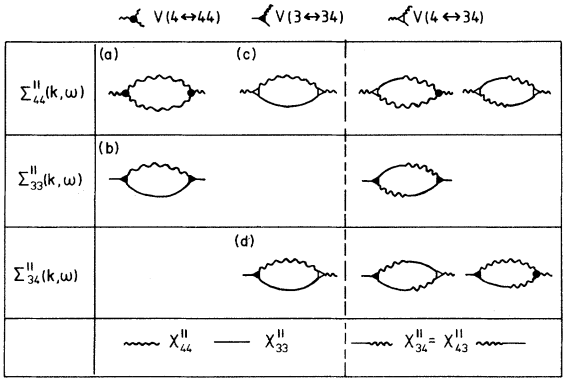

FIG. 5. Two-mode contributions (C6) to the self-energies $\Sigma''_{ij}(k,\omega)$ (C2) if vertices $V(4 \Longleftrightarrow 33), V(3 \Longleftrightarrow 33)$, $V(3 \Longleftrightarrow 44)$ are neglected.

are in the frequency range $\omega \lesssim \epsilon^0_4(k)$, still quite similar to those obtained in Sec. IV. For higher frequencies there are additional multimode contributions. Furthermmore, the peak widths of $\chi''_{ij}(k,\omega)$ at $\omega \simeq \epsilon^0_4(k)$ are now finite also outside the quasiparticle-quasihole band (4.12) due to decay into a $\rho_3\rho_4$ mode. However, the decay rate is rather small there (the full-width at half maximum is at most 0.05 K around the maxon) as a result of kinematic restriction[9] for diagrams (b)–(d) and the small vertex $V(4 \Longleftrightarrow 34)$. Of the diagrams in Fig. 5 only (c) and (d) and, to a lesser degree, (b), contribute to the finite life time of ^{4}He single-mode excitations. Except for the anomalous phonon dispersion the latter are stable,[12,26] at least in pure ^{4}He, against decay into two-mode excitations of ^{4}He since $\Sigma''^{0}_{44}(k,\omega)=0$ for $\omega \leq \epsilon^0_4(k)$.

The peak positions of $\chi''_{44}(k,\omega)$, $\chi''_{33}(k,\omega)$, and $S_{\mathrm{tot}}(k,\omega)$ are almost identical to those obtained in Sec. IV for $k \lesssim 1.75$ Å^{-1}, i.e., as long as the dominant ^{4}He mode lies outside the quasiparticle-hole band. Otherwise the two excitation energies $\epsilon^0_4(k)$ and $\epsilon^0_3(k)$ are so close that there is a strong level repulsion (see below) leading to a peak splitting in $\chi''_{33}(k,\omega)$ and in $\chi''_{44}(k,\omega)$, which is for $k=2$ Å^{-1} about 3.5 K compared to 1.8 K for χ''_{33} in Fig. 2. Owing to the level repulsion, considerable spectral weight of $\chi''_{33}(k,\omega)$ remains below the single-mode dispersion $\epsilon^0_4(k)$ even up to $k=2.25$ Å^{-1}. The lower peak positions of $\chi''_{33}(k,\omega)$ are similar to the solid triangles in Fig. 2. For $k \gtrsim 1.75$ Å^{-1}, however, they are shifted here to smaller frequencies as a result of the stronger level repulsion. The corresponding widths are rather small, $2\Gamma_{33}=0.15$ K (1.7 K) at $k=2$ Å^{-1} (2.25 Å^{-1}). At $k=2$ Å^{-1}, i.e., just above the level crossing, the intensities of the two peaks of $\chi''_{44}(k,\omega)$ are still almost equal

whereas at $k=2.25$ Å^{-1} more spectral weight is transferred to the upper peak. The width $2\Gamma_{44}=0.13$ K of the lower peak of $\chi''_{44}(k=2$ Å$^{-1},\omega)$ is practically determined by decay into ^{3}He quasiparticle-quasihole excitations since the two-mode dissipation spectrum Σ''^0_{33} is still zero for that frequency. However, for larger wave numbers, decay of a ^{4}He single mode into $\rho_3\rho_4$ excitations is kinematically possible thus causing broader widths than those following from decay into ^{3}He quasiparticle-hole excitations.

To understand the origin of the large frequency renormalization and peak splitting around $k=2$ Å^{-1} note that decay into two-mode excitations (i) hybridizes a ^{3}He or a ^{4}He density fluctuation with $\rho_3\rho_4$ by virtual transformation of the former into intermediate excitations of the latter [Figs. 5(b) and 5(c)], and (ii) it induces a direct dynamical decay interaction [Fig. 5(d)] between a ^{3}He and a ^{4}He density fluctuation by which the former is absorbed and the latter is generated and vice versa. Both processes cause frequency renormalization and peak splitting (here not only the off-diagonal elements of the restoring force matrix but also the off-diagonal self-energies induce coupling between the diagonal elements of restoring force and self-energy matrix), but mainly the latter is responsible for the too-large peak splitting. This numerically confirmed fact can be understood as follows. Both level repulsion induced by static coupling $W(k)$ and the hybridization of a ^{4}He single mode with a ^{3}He quasiparticle-quasihole excitation are small. Renormalization of the ^{3}He excitation frequency by the real part $\Sigma'^0_{33}(k,\omega)$ of Fig. 5(b) alone leads[9] to a ^{3}He quasiparticle dispersion which approaches $\epsilon^0_4(k)$ around roton wave numbers but does not induce a downward shift to about $0.85\epsilon^0_4(k)$ for $k=2.0$ Å^{-1}. So one is left with diagrams Figs. 5(c) and 5(d), both of their real parts having the frequency dependence of $\Sigma'^0_{33}(k,\omega)$. However, the off-diagonal element of the self-energy matrix (C11) due to Fig. 5(d) enters the determinant of the inverse reponse matrix with twice as large a weight as the diagonal element due to Fig. 5(c).

In technical terms the origin of the large level repulsion is the too-large real part $\Sigma'_{34}(k,\omega\simeq\epsilon^0_4(k))$ around the level crossing at $\epsilon^0_4(k)$. That in turn is a result of the too-large positive spectral weight in the dissipation spectrum from Fig. 5(d). In contrast to the contribution $\sim\Sigma''^0_{33}(k,\omega)$ of the latter, the exact spectrum $\Sigma''_{34}(k,\omega)$ is indefinite for $\omega>0$; i.e., it changes sign and can thus be expected to have a smaller real part. Note that the last two diagrams of Fig. 5 contributing to $\Sigma''_{34}(k,\omega)$ can decrease the spectral weight since their contributions are indefinite with $\chi''_{34}(k,\omega)$ being indefinite. Thus in this appendix we have discarded decay channels which should have been kept, and furthermore have not performed a fully self-consistent calculation; both are the subject of future work. Although this will change the spectra, we nevertheless included this appendix to elucidate some aspects of the influence of two-mode decay and to show how intricate the problems of hybridization with two-mode excitations are.

---

[1]We use the word spectrum for the Fourier transform of a correlation or response function and the word dispersion for the wave-number dependence of a particular peak thereof.

[2]L. D. Landau and I. Ya. Pomeranchuk, Dokl. Akad. Nauk Uzb. 59, 669 (1948); I. Ya. Pomeranchuk, Zh. Eksp. Teor. Fiz. 19, 42 (1949).

[3]N. R. Brubaker, D. O. Edwards, R. E. Sarwinski, P. Seligmann, and R. A. Sherlock, Phys. Rev. Lett. 25, 715 (1970); J. Low Temp. Phys. 3, 619 (1970).

[4]L. P. Pitaevskij (unpublished); M. J. Stephen and L. Mittag, Phys. Rev. Lett. 31, 923 (1973); C. M. Varma, Phys. Lett. 45A, 301 (1973); V. I. Sobolev and B. N. Esel'son, Zh. Eksp. Teor. Fiz. Pis'ma Red. 18, 689 (1973) [JETP Lett. 18, 403 (1973)].

[5]B. N. Esel'son, V. A. Slyusarev, V. I. Sobolev, and M. A. Strzhemechnyi, Zh. Eksp. Teor. Fiz. Pis'ma Red. 21, 253 (1975) [JETP Lett. 21, 115 (1975)].

[6]R. B. Kummer, V. Narayanamurti, and R. C. Dynes, Phys. Rev. B 16, 1046 (1977).

[7]J. Ruvalds, J. Slinkman, A. K. Rajagopal, and A. Bagchi, Phys. Rev. B 16, 2047 (1977); J. Ruvalds, in *Quantum Liquids,* edited by J. Ruvalds and T. Regge (North-Holland, Amsterdam, 1978), pp. 263–291.

[8]D. S. Greywall, Phys. Rev. Lett. 41, 177 (1978); Phys. Rev. B 20, 2643 (1979).

[9]W. Götze, M. Lücke, and A. Szprynger, J. Phys. (Paris) C6, 196 (1978); Phys. Rev. B 19, 206 (1979).

[10]R. N. Bhatt, Phys. Rev. B 18, 2108 (1978).

[11]Throughout this work a superscript 0 either identifies a property of pure ^{4}He or a quantity related to a single ^{3}He atom in ^{4}He.

[12]M. Lücke, in *Lecture Notes in Physics,* edited by A. Pekalski and J. Przystawa (Springer, Berlin, 1980), Vol. 115.

[13]N. E. Dyumin, B. N. Esel'son, E. Ya. Rudavskii, and I. A. Serbin, Zh. Eksp. Teor. Fiz. 56, 747 (1969) [Sov. Phys.—JETP 29, 406 (1969)]; B. N. Esel'son,

Yu. Z. Kovdrya, and V. B. Shikin, *ibid.* 59, 64 (1970) [*ibid.* 32, 37 (1971)]; V. I. Sobolev and B. N. Esel'son, *ibid.* 60, 240 (1971) [*ibid.* 33, 132 (1971)].

[14]C. M. Surko and R. E. Slusher, Phys. Rev. Lett. 30, 1111 (1973); R. L. Woerner, D. A. Rockwell, and T. J. Greytak, *ibid.* 30, 1114 (1973).

[15]J. M. Rowe, D. L. Price, and G. E. Ostrowski, Phys. Rev. Lett. 31, 510 (1973).

[16]P. A. Hilton, R. Scherm, and W. G. Stirling, J. Low Temp. Phys. 27, 851 (1977).

[17]D. L. Bartley, J. E. Robinson, and V. K. Wong, J. Low Temp. Phys. 12, 71 (1973); D. L. Bartley, V. K. Wong, and J. E. Robinson, *ibid.* 17, 551 (1974).

[18]The Neutron Diffraction Commission, Acta Crystallogr. A25, 391 (1969).

[19]P. C. Martin, in *Problème à N Corps,* edited by C. de Witt and R. Balian (Gordon and Breach, New York, 1968).

[20]D. Forster, *Hydrodynamic Fluctuations, Broken Symmetry, and Correlation Functions* (Benjamin, Reading, Massachusetts, 1975).

[21]R. A. Cowley and A. D. B. Woods, Can. J. Phys. 49, 177 (1971); A. D. B. Woods and R. A. Cowley, Rep. Prog. Phys. 36, 1135 (1973).

[22]D. Pines and P. Nozières, *The Theory of Quantum Liquids* (Benjamin, New York, 1966).

[23]H. Mori, Prog. Theor. Phys. 33, 423 (1965); 34, 399 (1965).

[24]M. Lücke and A. Szprynger, Physica 107B, 33 (1981).

[25]P. A. Hilton, R. Scherm, and G. W. Stirling (unpublished).

[26]W. Götze and M. Lücke, Phys. Rev. B 13, 3825 (1976).

[27]To be precise (see Refs. 9 and 12) the excitation spectrum consists of a δ function at $\omega=\epsilon_3^0(k)$ and a hybridization continuum at larger frequencies. The undamped ^{3}He quasiparticle excitation carries for wave numbers up to about 2 Å^{-1} a fraction $\frac{1}{2}\lesssim f_3^0(k)\leq 1$ of the total spectral weight (Ref. 9).

[28]N. W. Ashcroft and N. D. Mermin, *Solid State Physics* (Holt, Rinehart and Winston, New York, 1976).

[29]A. L. Fetter and J. D. Walecka, *Quantum Theory of Many-Particle Systems* (McGraw-Hill, New York, 1971).

[30]R. Scherm, W. G. Stirling, and P. A. Hilton J. Phys. (Paris) C6, 198 (1978).

[31]W. E. Massey, C. W. Woo, and H. T. Tan, Phys. Rev. A 1, 519 (1970).

[32]H. T. Tan and C. W. Woo, Phys. Rev. A 7, 233 (1973).

[33]M. Suemitsu and Y. Sawada, Phys. Lett. 71A, 71 (1979).

[34]E. K. Achter and L. Meyer, Phys. Rev. 188, 291 (1969).

[35]R. B. Hallock, Phys. Rev. A 5, 320 (1972).

[36]J. Bosse, W. Götze, and M. Lücke, Phys. Rev. A 17, 434 (1978).

[37]J. P. Boon and S. Yip, *Molecular Hydrodynamics* (McGraw-Hill, New York, 1980).

[38]$S_{34}(k)$ in (2.13) of Ref. 9 does not denote the ^{3}He-He II structure factor as stated there but rather

$$n_4\int d\vec{r}\,e^{-i\vec{k}\cdot\vec{r}}\,[g_{34}(r)-1]=S_{34}(k)\sqrt{n_4/n_3}.$$